Letter to the Editor

A MORPHOLOGICAL METHOD TO DETERMINE CO-ROTATION RADII IN SPIRAL GALAXIES

Ivânio Puerari

Instituto Nacional de Astrofísica, Óptica y Electrónica, Apartado Postal 216, 72000 Puebla, Mexico

and

Horacio Dottori

Departamento de Astronomia, Instituto de Física, UFRGS, CxP 15051, CEP 91501-907 Porto Alegre, Brazil

Received ______________________; accepted ______________________

ABSTRACT

Shock induced star formation in a stellar density wave scenario produces an azimuthal gradient of ages across the spiral arms which has opposite signs on either side of the corotation resonance (CR). We present a method based on the Fourier analysis of azimuthal profiles, to locate the CR and determine the arm character (trailing or leading) in spiral galaxies. Basically, we compare the behavior of the phase angle of the two-armed spiral in blue and infrared colors which pick out respectively young and older disk stellar population. We illustrate the method using theoretical leading and trailing, spirals. We have also applied the method to the spiral galaxies NGC 7479, for which we confirm the reported leading arms, and NGC 1832. In these galaxies we find two and three CRs respectively.

Subject headings: galaxies: spiral – galaxies: kinematics and dynamics – galaxies: individual (NGC 1832, NGC 7479) – method: analytical

Introduction

Schweizer (1976) and Beckman & Cepa (1990, hereinafter BC90) have previously discussed what would be the behavior of the colors across spiral arms if a shock generated by a spiral density wave (SDW) induces star formation. The main azimuthal observable characteristics of this scenario are steeper azimuthal profiles and bluer color indexes on the side where the shock front is located. Elmegreen, Elmegreen & Montenegro (1992) also pointed out that such evidence for the CR is clear in gas-rich galaxies in the form of sharp endpoints to star formation ridges and dust lanes in two arm spirals.

BC90 analyzed azimuthal profiles of the spiral galaxies NGC 7479 and NGC 1832, detecting a systematic shift between the arm phase in B and I colors. For the B band, OB stars represent 70% of the luminosity and the older stars of the disk only 30%. For the I band, most of the contribution (80%) is due to disk stars (Schweizer 1976). Then, within the framework of the SDW theory, BC90 have basically detected the relative position of the shock front with respect to the SDW perturbation. In a previous paper (Puerari & Dottori, 1992), we proposed a method to determine the leading or trailing character of perturbation in spiral galaxies by analyzing the distribution of HII regions. We present in this *Letter* a useful method to locate CR and to determine the leading or trailing character of a perturbing pattern. It is based on the analysis of azimuthal profiles of two-armed spiral galaxies by means of Fourier transforms applied to B and I images.

The method is described in the next section, where we also analyze ideal spirals, and show the behavior of the phase Θ in the θ vs r diagrams, suitable to be compared directly with those of true spiral galaxies. In Sect. 3 we discuss the case of NGC 7479, reported as a leading spiral (BC90), and that of NGC 1832. Finally, our conclusions are given in Sect. 4.

The method

Shock induced star formation in a stellar density wave scenario produces an azimuthal spread of ages across the spiral arms. At the corotation radius (CR) the angular velocity of the perturbation (Ω_p) and that of the stellar disk (Ω) coincide. A comoving observer at the CR will see out- and inwards, the shock front to change from one side of the spiral to the other, consequently reversing the order in which young and older disk stellar populations appear in azimuthal profiles across the arm. In order to detect the shock front jump, we analyze the relative behavior of the SDW and shock front phases, Θ_{dw} and Θ_{sf} respectively, by means of the Fourier transform of azimuthal profiles $I_r(\theta)$ given by,

$$\mathcal{F}_2(r) = \int_{-\pi}^{\pi} I_r(\theta) e^{-2i\theta} d\theta$$

The phase Θ can be obtained as,

$$\Theta(r) = \tan^{-1} \frac{Re[\mathcal{F}_2(r)]}{Im[\mathcal{F}_2(r)]}$$

where Re and Im mean the real and imaginary part of the complex Fourier coefficient.

In Figs. 1a to 1d, we show idealized two-armed spirals of leading and trailing character, and on-the-sky views of types S and Z. The light line represents the SDW and the heavy line the shock front. Figs. 2a to 2d show the relative behavior of $\Theta_{sf}(r)$ and $\Theta_{dw}(r)$ for the four cases of Fig. 1. As can be seen, the position of the CR and the trailing or leading character of the arms are clearly revealed in these plots.

Analysis of NGC 1832 and NGC 7479

Frames are oriented with N at the top and E to the left. The azimuthal profiles are obtained counterclockwise, beginning at the South.

The B and I frames of NGC 1832 images are the same as those used in BC90. NGC 7479 images have been obtained later on, also with the J. Kapteyn telescope, at the Roque de los Muchachos Observatory in La Palma, with a larger CCD, which allowed the whole galaxy to be imaged (The images were kindly provided by J. Cepa).

Photometrically calibrated frames are not required to carry out the phase analysis, but it was necessary to eliminate all the stars from the frames and to deproject the galaxies.

Following the discussion of the two previous sections, the curves $\Theta_B(r)$ and $\Theta_I(r)$ are respectively equivalent to Θ_{sf} and Θ_{dw}.

NGC 7479 presents an on-the-sky view of Z-type . The curves $\Theta_B(r)$ and $\Theta_I(r)$ (Fig. 3), intercept at $r \approx 55$", which coincides with the CR position given by BC90. The relative position of the curves is comparable to that of Fig. 2c, which confirms, consequently, the leading character of the pattern with CR at the end of the bar. A second intersection is present at $r \approx 23$", that time indicating a trailing pattern. As Fig. 4 shows, the outer CR lies on the northern extreme of the bar and is about 20% outwards from the southern one. Fig. 4 also shows that the inner CR bounds the fat internal part of the bar, and marks a cut in the fine internal dust lane that comes out of the nucleus. These features are signatures of a CR, as pointed out by Elmegreen, Elmegreen & Montenegro (1992). The presence of a second CR inside a rigid bar might be due to the perturbation of the velocity field caused by the strong mass inflow, with speed as high as 20 km/sec (Quillen et al. 1995). It is important to point out, as numerical simulations show, that a inflow speed as high as this is consistent with the predictions of galaxy mergers (Mihos & Hernquist 1994a,b) and not with that of a bar perturbation in an isolated galaxy (Athanassoula 1992, 1-6 km/sec). Beckman suggests that there could exist a trailing solution for NGC 7479 also. However, Beckman realized this scenario is not easy to verify. Since we have not found a third CR, like that in NGC 1832 (see Fig. 7), Beckman's claim would require that $\Omega_p(r) \leq \Omega(r)$ for $r \geq R_{CR_2}$. Spatially larger and deeper images would be necessary in order to check the existence of a third CR beyond the limits of the images used in this paper.

NGC 1832 presents an on-the-sky view of S-type. The curves $\Theta_B(r)$ and $\Theta_I(r)$ (Fig. 5) present three intersections. This plot also shows that the structure inside the ring ($r \leq 17$") is not precisely a bar, but an arm-like structure, with a winding opposite to the external arms. The first intersection indicate a CR coincident with the internal border of the ring ($r \approx 15$", Fig. 6). The second and third CRs, mark gaps in the strong eastern arm and the broadening and bifurcation of the western one. The inner and the outer CRs indicate leading patterns, and the intermediate CR a trailing one. In Fig. 7 we show schematically,

the relative behavior of the disk and the perturbing pattern angular velocities.

The errors in the determination of the CRs are difficult to evaluate in real cases and to estimate by models such as those of Fig. 1. Factors that may affect this determination are the departure from 180° symmetry of the two arms structure, differences between the brightness of the two arms, the pitch angle (bars, and open arms will give more reliable results that closed ones), the arm width, etc. At all events, we suggest that the method should not be applied to galaxies with inclination larger than 55° to 60°.

Conclusions

We present a method to locate the CR and determine the trailing or leading character of the spiral pattern in two-armed spiral galaxies, based on the Fourier transform of azimuthal profiles in B and I images.

We present also theoretical plots of the relative behavior of the phase angles $\Theta_B(r)$ and $\Theta_I(r)$ in the θ vs r plane, for trailing and leading spirals that show up as S- or Z-type, useful to easily and quickly check the result when applying this method to real spiral galaxies.

We confirm for NGC 7479 the existence of the leading pattern with CR at the extreme of the bar. We found in this galaxy the existence of a internal CR, indicating a trailing pattern.

NGC 1832 presents three CRs, the inner and the outer ones indicate leading pattern and the intermediate CR a trailing one. The most plausible physical interpretation for this situation is the existence of two pattern speeds.

The continuity of the curves Θ_B and Θ_I in both galaxies might be indicating that trailing and leading phenomena are physically related in these objects. A larger sample of galaxies is being analyzed.

We acknowledge Dr. Beckman for helpful suggestions about the interpretation of the phase diagrams specially for Figure 7. This work is being partially supported by the brazilian institution CNPq and CAPES and CONACYT from Mexico.

REFERENCES

Athanassoula, E. 1992, MNRAS, 259, 345

Beckman, J. E., Cepa, J. 1990, A&A, 229, 37

Elmegreen, B. G. 1991, in Dynamics of Galaxies and their Molecular Cloud distribution, ed. F. Combes & F. Casoli (Dordrecht: Kluwer), 113

Elmegreen, B. G., Elmegreen, D. M., Montenegro, L. 1992, ApJS, 79, 37

Elmegreen, D. M., Elmegreen, B. G. 1995, ApJ, 445, 591

Mihos, J. C., Hernquist, L. 1994a, ApJ, 425, L13

Mihos, J. C., Hernquist, L. 1994b, ApJ, 431, L9

Puerari, I., Dottori, H. 1992, A&AS, 93, 469

Quillen, A. C., Frogel, J. A., Kenney, J. D. P., Pogge, R. W., DePoy, D. L. 1995, ApJ, 441, 549

Schweizer, F. 1976, ApJS, 31, 313

This manuscript was prepared with the AAS LaTeX macros v4.0.

Fig. 1.— The position of the shock front (heavy line) with respect to the SDW (light line) for a: a- leading, S-type; b- trailing, S-type; c-leading, Z-type; d- trailing, Z-type wave. The arrow in each panel indicates the sense of the disc rotation. Note: An S-type object would be seen as Z-type if viewed from the opposite pole of its axis of rotation. The distinction is observational rather than physical.

Fig. 2.— Relative behavior of the phase $\Theta(r)$ of the SDW (dashed line) and the shock front (full line) for the four cases of Fig. 1.

Fig. 3.— Relative behavior of the two arm phase $\Theta_B(r)$ and $\Theta_I(r)$ for NGC 7479. The diagram indicates the presence of two CRs at $r \approx 23$" and $r \approx 55$". The SDW is trailing around the inner CR and leading around the outer one.

Fig. 4.— CR circles on NGC 7479 B image. N at the top and E to the left. Scales are in pixels, 1 pxl=0.560", V_R=2378 km/sec.

Fig. 5.— Relative behavior of the phases $\Theta_B(r)$ and $\Theta_I(r)$ for NGC 1832. The diagram indicates the presence of three CRs at $r \approx 15$", $r \approx 34$", and $r \approx 40$". The SDW is leading around the inner and the outer CRs and it is trailing around the intermediate one.

Fig. 6.— B image of NGC 1832 showing the position of the three CRs. N at the top and E to the left. Scales are in pixels, 1 pxl=0.414", V_R=1937 km/sec.

Fig. 7.— We show schematically for NGC 1832, the possible relative behavior of the disk (full line) and the perturbing pattern (dashed line) angular velocities.

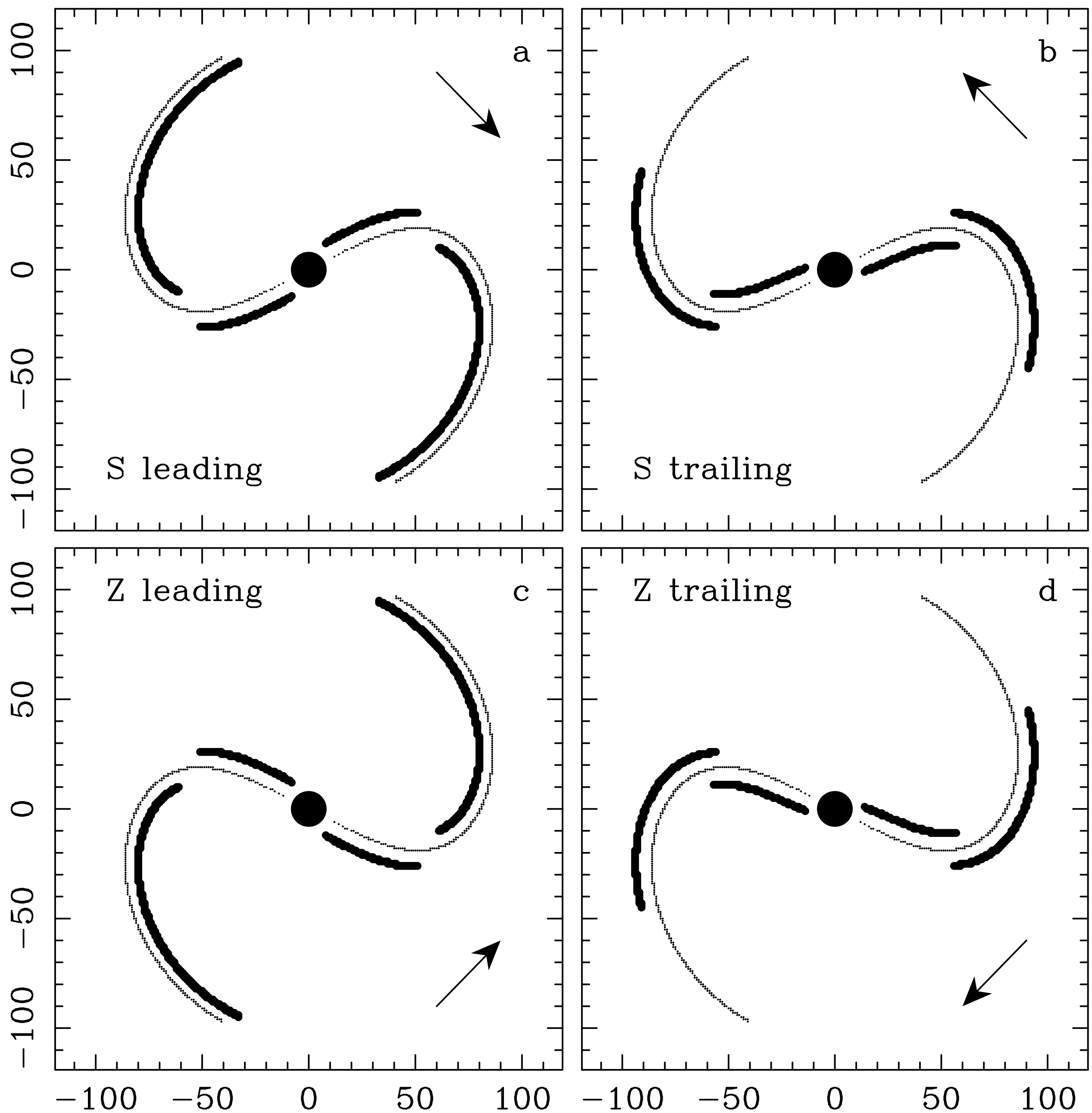

a
S leading
b
S trailing
c
Z leading
d
Z trailing
100
50
0
−50
−100
−100
−50
0
50
100

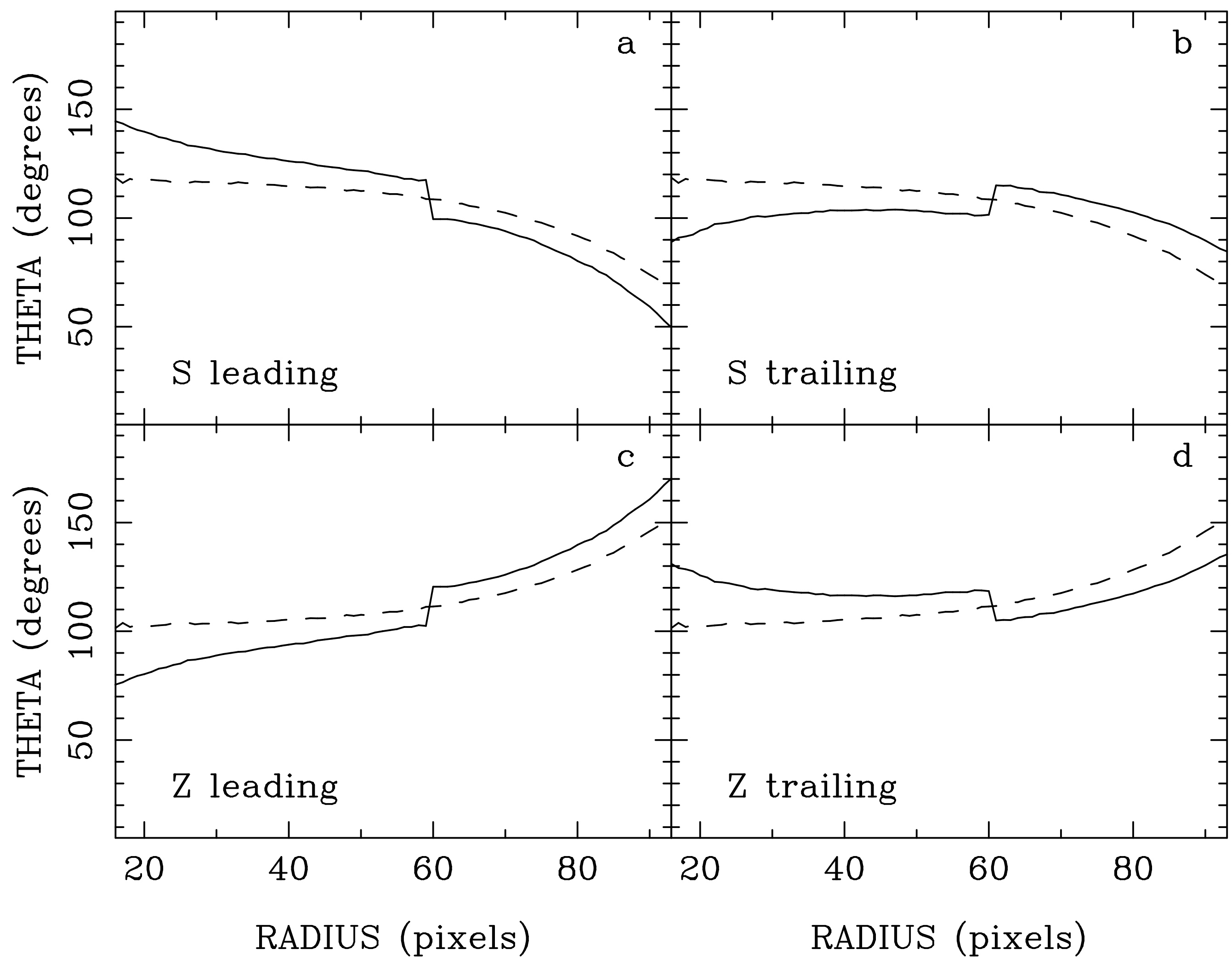
a
b
c
d
S leading
S trailing
Z leading
Z trailing
THETA (degrees)
THETA (degrees)
RADIUS (pixels)
RADIUS (pixels)
150
100
50
150
100
50
20
40
60
80
20
40
60
80

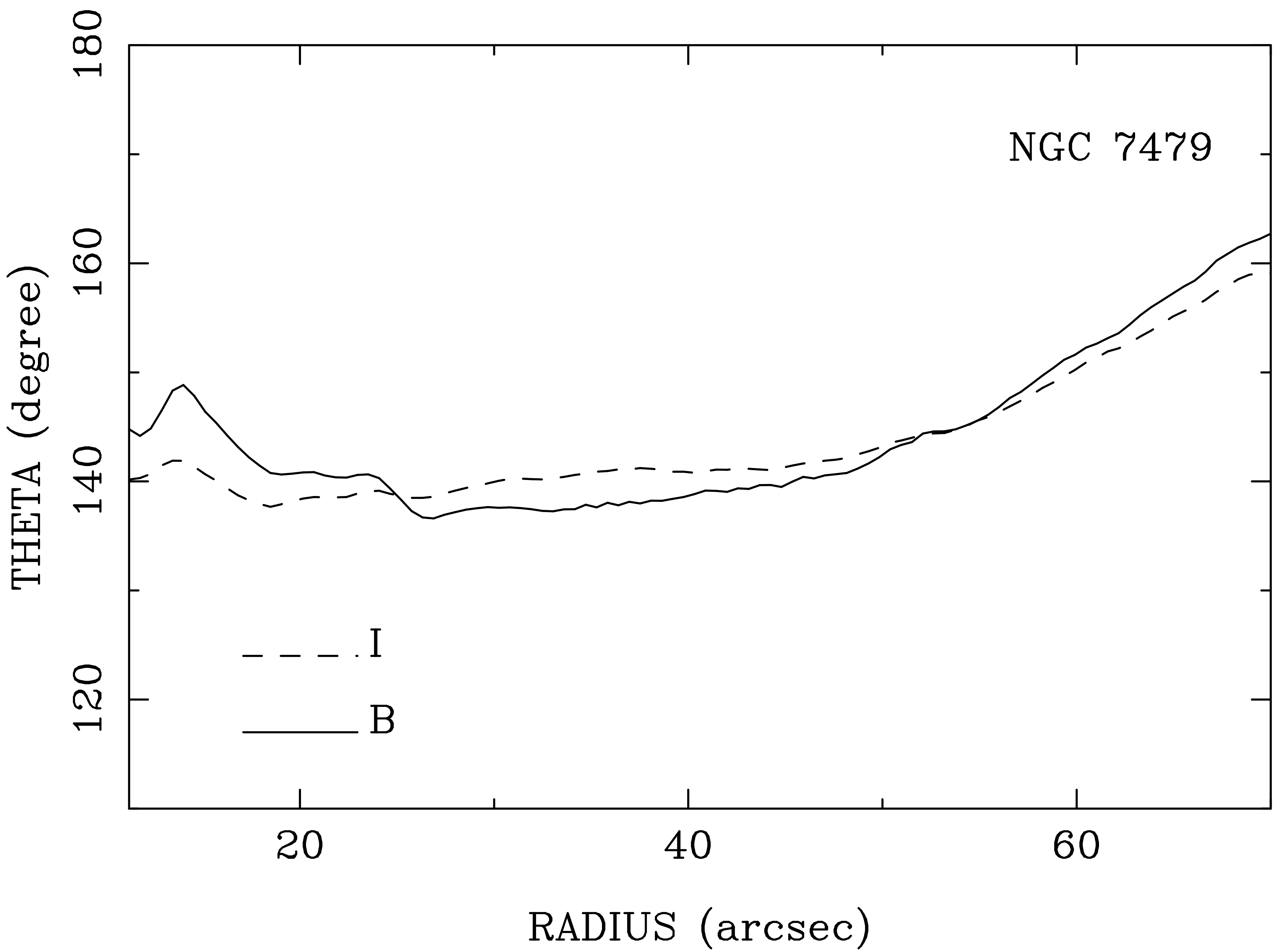
NGC 7479
THETA (degree)
180
160
140
120
20
40
60
RADIUS (arcsec)
I
B

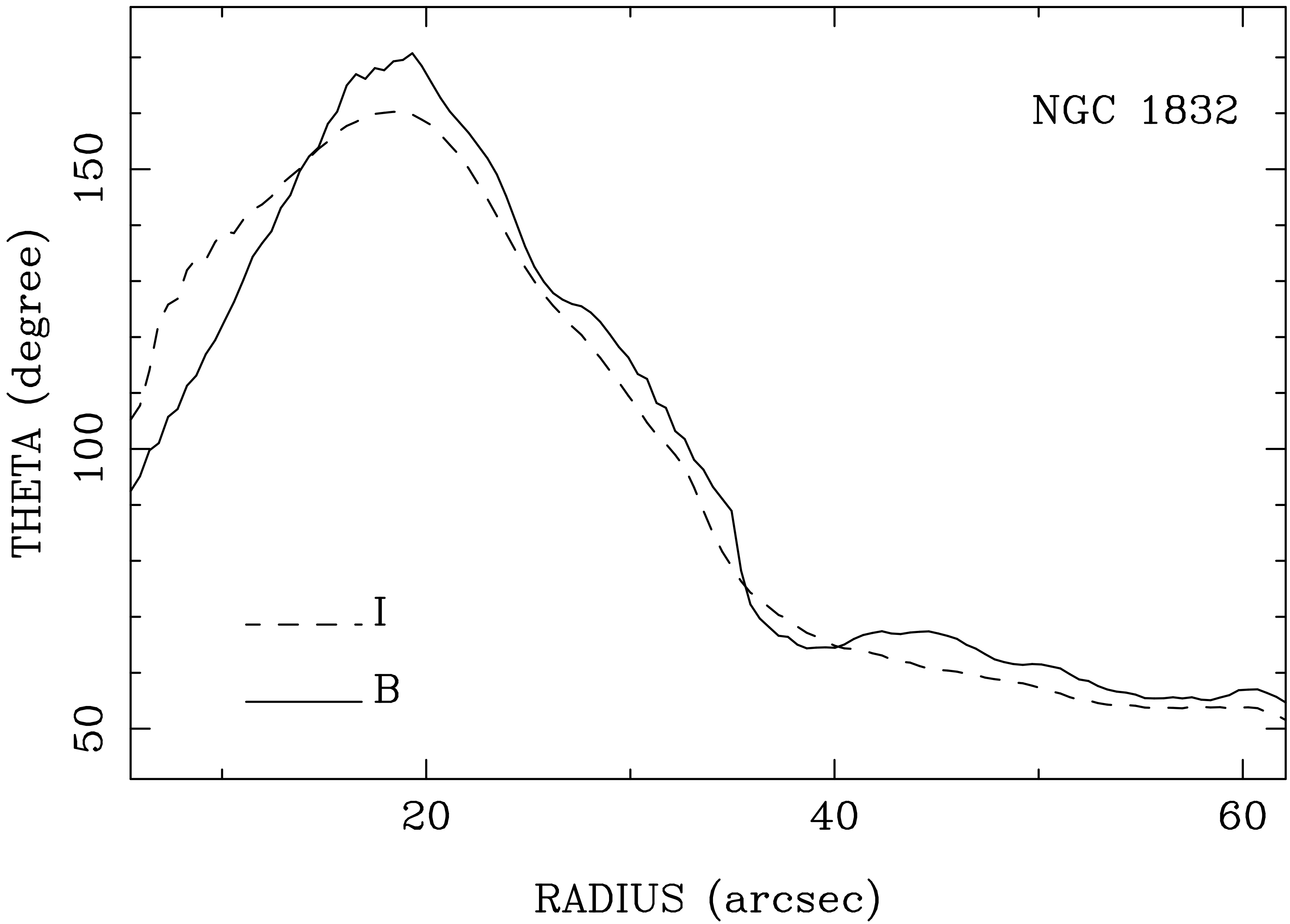
NGC 1832
I
B
THETA (degree)
150
100
50
RADIUS (arcsec)
20
40
60

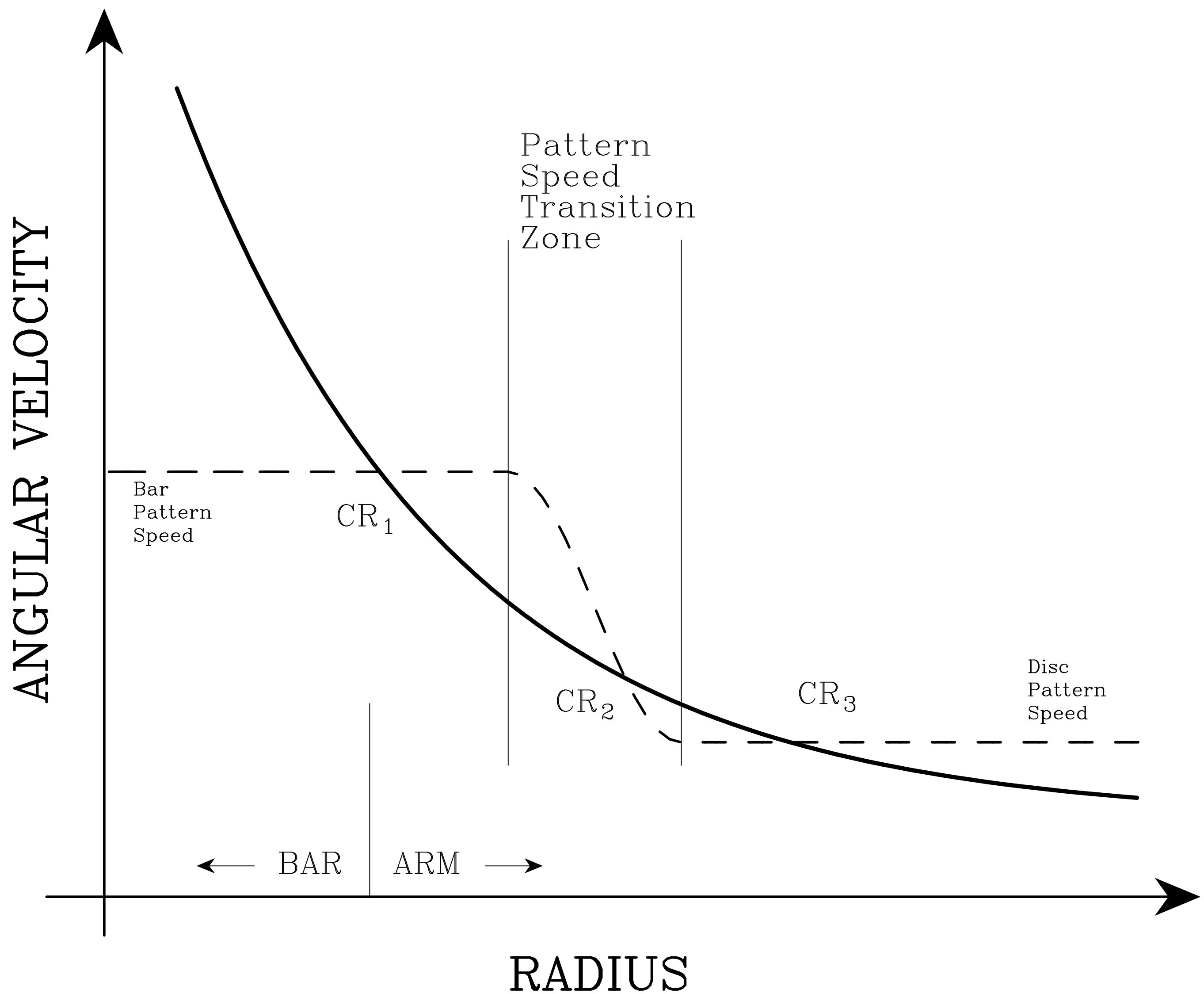
ANGULAR VELOCITY
RADIUS
Pattern Speed Transition Zone
Bar Pattern Speed
Disc Pattern Speed
CR1
CR2
CR3
BAR
ARM